Light-based feedback for controlling intracellular signaling dynamics

Jared E Toettcher[1,2], Delquin Gong[1], Wendell A Lim[2,3] & Orion D Weiner[1]

The ability to apply precise inputs to signaling species in live cells would be transformative for interrogating and understanding complex cell-signaling systems. Here we report an 'optogenetic' method for applying custom signaling inputs using feedback control of a light-gated protein-protein interaction. We applied this strategy to perturb protein localization and phosphoinositide 3-kinase activity, generating time-varying signals and clamping signals to buffer against cell-to-cell variability or changes in pathway activity.

To dissect how cell signaling networks sense, encode and process information, we need not only a parts list but also an understanding of how their constituent molecular components vary over time in response to diverse input signals. One powerful set of approaches for interrogating cellular circuits combines controlled, time-varying perturbations with live-cell signaling readouts[1–3]. This can be used to analyze how a pathway maps diverse inputs to outputs and to distinguish the nature, timescale and strength of feedback connections in a biological network.

Genetically encoded light-gated proteins are a promising technology (optogenetics) for delivering precise intracellular inputs to individual cells. However, their broad application faces three challenges. First, cells have variable expression of optogenetic-system components, so the same light input will result in different activity across a population of cells. Second, even in an individual cell, the relationship between light input and activity can be complex and nonlinear. Thus, it is very difficult to identify how the amount of light should be varied to drive a defined time course of intracellular activation. Finally, many signaling pathways incorporate regulatory connections whose strength varies over time. Even obtaining constant pathway activity can require time-varying light inputs that compensate for intracellular feedback.

In this study we address these challenges by coupling a tunable optogenetic module with automated control of light input (**Fig. 1a**). Using live-cell measurements of intracellular activation to update light levels in real time, we implemented a computational feedback controller to act as a 'concentration clamp', analogous to voltage clamping for neuron excitation[4] or positional clamping[5] for mechanical systems. Our controller can drive precise activity levels that vary with time, automatically identifying the light input required to correct for a nonlinear light-activity relationship. It can deliver custom amounts of light to each cell in a population to compensate for cell-to-cell variability in optogenetic-component expression. Finally, the controller can be used to clamp a downstream signaling node at a defined level, even when the node is affected by additional regulatory inputs over time. We focused on light-gated recruitment of residues 1–100 of phytochrome-interacting factor 6 (PIF6) to residues 1–908 of PhyB (Phy)[6,7] to direct membrane translocation of signaling proteins in mammalian cells[8] (**Fig. 1a**). Phy-PIF modules have been used for light-gated regulation of diverse biological processes[9–11]. We applied different ratios of 650-nm and 750-nm light to specific regions of live cells to titrate the recruitment of a fluorescently tagged PIF fusion protein, PIF-BFP, to the membrane (Online Methods and **Supplementary Fig. 1**).

We first implemented a feedback control system that can generate user-defined dynamics of PIF-tagged protein recruitment to the plasma membrane (**Fig. 1b**). In this system, the user provides a desired activity time course (target function) that the controller compares to a measured live-cell activity readout (output) in real time to determine the appropriate light input to provide to the cell. The Phy-PIF system is well suited for such a strategy because its binding is switchable on a timescale of seconds, and PIF membrane translocation can be directly measured in live cells. We based our feedback controller on a widely used architecture, proportional-integral control, because it can drive precise outputs without requiring a detailed model of the system and is robust to measurement noise (**Supplementary Note 1**). After validating the control strategy by applying it to a fitted mathematical model of Phy-PIF–based membrane translocation (**Supplementary Figs. 2–5**), we implemented it experimentally using custom Matlab and Micro-Manager[12] code (**Supplementary Software 1**) to acquire images, measure the extent of membrane PIF recruitment and automatically adjust intensity of the 650-nm LED.

We used the controller to set a constant level of PIF-BFP membrane recruitment. Before starting the controller, we initialized the Phy-PIF system to an 'off' state by exposure to 750-nm light. During each control time course, we measured the extent of recruitment and used it to update the light input once per second. Using this strategy we could drive membrane recruitment of PIF-tagged proteins to desired levels within seconds across a range of feedback strengths and sampling times (**Fig. 1c** and **Supplementary Fig. 6a**,**b**).

We next tested whether we could extend our feedback-control system to generate user-defined time-varying inputs.

[1]Cardiovascular Research Institute and Department of Biochemistry, University of California San Francisco, San Francisco, California, USA. [2]Department of Cellular and Molecular Pharmacology, University of California San Francisco, San Francisco, California, USA. [3]Howard Hughes Medical Institute, University of California San Francisco, San Francisco, California, USA. Correspondence should be addressed to O.D.W. (orion.weiner@ucsf.edu) or W.A.L. (lim@cmp.ucsf.edu).

RECEIVED 11 APRIL; ACCEPTED 4 AUGUST; PUBLISHED ONLINE 11 SEPTEMBER 2011; DOI:10.1038/NMETH.1700

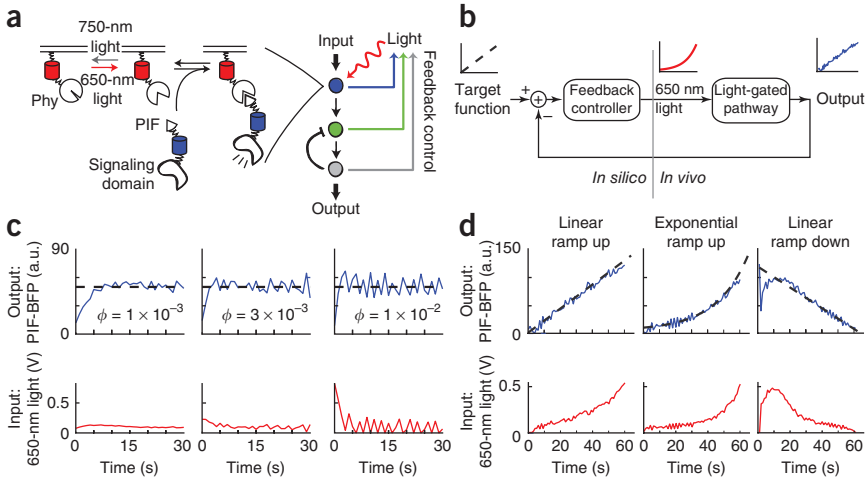

Figure 1 | Feedback control to modulate plasma-membrane recruitment of PIF-tagged inputs. (**a**) Schematic of feedback control of the Phy-PIF optogenetic module. Upon ligation to the small-molecule chromophore phycocyanobilin (PCB), membrane-fused, fluorescent Phy fusion proteins can be used to drive fluorescent PIF-tagged proteins to the plasma membrane by exposure to 650-nm light, and this interaction can be reversed by exposure to 750-nm light. By automatically tuning input light levels, feedback control sets the activity state at downstream nodes for which live-cell readouts are available. (**b**) Schematic of the feedback control system. The user specifies a target function, which is compared to live-cell measurements of intracellular activity (output). The resulting error signal is supplied to the feedback controller to determine the proper light input to an optogenetically gated intracellular signal. (**c**,**d**) Feedback control of Phy-PIF binding in individual live cells to constant (**c**) or time-varying (**d**) membrane binding. The controller drives membrane binding (top) to a desired trajectory (target function; dashed black lines) by adjusting 650-nm LED voltage (bottom). ϕ, feedback strength. PIF-BFP membrane binding (labeled PIF-BFP) is shown in arbitrary units (a.u.).

Using microfluidics, ramped inputs have been used to dissect sensory adaptation[2,3], and oscillating inputs have uncovered feedback loops modulating signal-transduction cascades[1]. However, previously it has not been possible to drive time-varying intracellular signals. We extended our controller to track time-varying target functions using a simple predictive control strategy: by comparing the observed membrane recruitment to the next time point's target level, the controller can anticipate how to change the amount of light to track a desired output without introducing a delay. In this mode, the controller could track precise temporal patterns of plasma-membrane recruitment, including linear and exponential ramps with varying steepness (**Fig. 1d** and **Supplementary Fig. 6c**). Even when initialized far from steady state (for example, with no light input but maximum PIF recruitment), the controller quickly converged on a target curve of PIF recruitment and maintained a faithful trajectory thereafter (**Fig. 1d**). Thus it is possible to drive dynamics of intracellular activity on a timescale of seconds, typically only achieved using extracellular inputs.

We next asked whether our control system could be used to compensate for cell-to-cell variability in recruitment resulting from nonuniform expression of optogenetic-system components (**Fig. 2a**). We measured PIF recruitment (**Fig. 2b**) and Phy-PIF expression (**Supplementary Fig. 7**) in 80 cells to characterize the extent of cell-to-cell variability. Because of variation in Phy-PIF expression, delivering the same light input across the population led to a broad distribution of PIF-BFP membrane recruitment. In contrast, the feedback controller tightened the distribution around a desired amount of PIF-BFP membrane recruitment by applying appropriate light inputs to each cell (**Fig. 2b**,**c**). Application of this technique decreased the cell population's s.d. of PIF recruitment fourfold, but the mean value of PIF recruitment was approximately unchanged (**Fig. 2d**,**e**). Thus, optogenetics-based feedback control can be used to tune recruitment levels in individual cells and reshape population-level distributions of intracellular activity.

In addition to directly controlling PIF-tagged inputs, feedback control can, in principle, be applied to downstream signals for which live-cell readouts are available. Because far more live-cell reporters are available than optogenetic inputs, this technique has the potential to greatly expand the number of signaling steps that can be readily placed under light control. To test this hypothesis, we focused on feedback control of the product of an enzymatic reaction in live cells: 3′ phosphoinositides generated by phosphoinositide 3-kinase (PI3K). We engineered optogenetic control of 3′ phosphoinositide lipid production using a strategy based on previous ones with

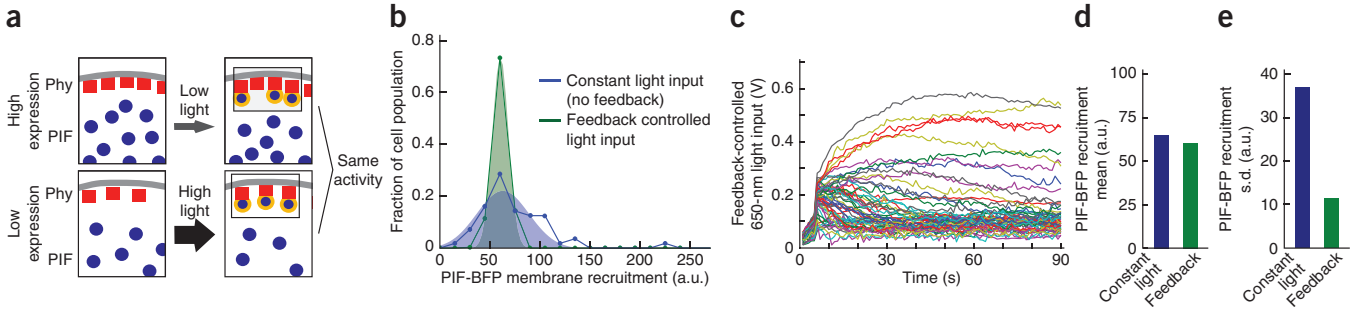

Figure 2 | Feedback control can decrease cell-to-cell variability in the optogenetic response. (**a**) Schematic of how different light inputs must be applied to drive the same recruitment in cells expressing different amounts of optogenetic components. (**b**) Histograms of PIF membrane recruitment under a constant light input (simultaneous illumination with 0.2 V, 650-nm light and 0.1 V, 750-nm light) and during feedback control. (**c**) The feedback-controlled voltages applied over time to each cell in **b**, showing that light inputs required to compensate for cell-to-cell heterogeneity span a large range of intensities. (**d**,**e**) The mean (**d**) and s.d. (**e**) of PIF recruitment in the presence or absence of feedback control for the cell populations shown in **b**.

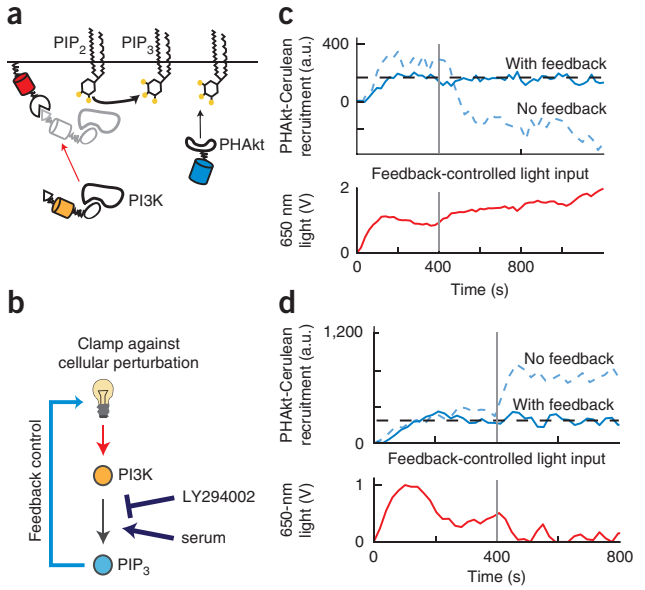

Figure 3 | Feedback control can clamp PIP_3 levels against cellular perturbations. (**a**) Schematic of PI3K recruitment to a membrane target (Phy-mCherry-CAAX) using a fluorescent PIF fusion protein (iSH-YFP-PIF) that constitutively binds endogenous PI3K. The 3′ phosphoinositide lipid amounts were assayed by measuring PHAkt-Cerulean recruitment to the plasma membrane. (**b**) Schematic of feedback control used to clamp perturbations in upstream signaling nodes by adjusting light levels to compensate for these changes (such as LY294002-based PI3K inhibition or serum-based PI3K activation). (**c**,**d**) Single-cell time courses in response to a constant light input or with feedback control (top graphs). At 400 s, 3′ phosphoinositide lipid production was perturbed (gray line) by addition of 1 μm LY294002 (PI3K inhibitor; **c**) or 10% serum (PI3K activator; **d**). Time-varying light input used by the feedback controller to clamp 3′ phosphoinositide lipid amounts (bottom graphs). Dashed lines indicate the target function.

chemical dimerizers to drive PI3K membrane recruitment[13]. In this system, a light-gated, fluorescent PI3K-binding domain (iSH-YFP-PIF; iSH is the inter-SH2 domain of p85) induces PI3K activity at specific regions of the cell membrane (**Fig. 3a** and **Supplementary Figs. 8** and **9**). This signaling process has the advantage of live-cell biosensors at two nodes: visualizing light-gated PI3K membrane recruitment and monitoring PI3K lipid products by the membrane translocation of a fluorescent Akt-PH domain (PHAkt-Cerulean, which binds to $PI(3,4)P_2$ and $PI(3,4,5)P_3$)[14]. Confirming our hypothesis that feedback control can be applied at sequential signaling nodes, we clamped upstream recruitment of PIF-tagged proteins (**Fig. 1c**,**d**) or downstream signals such as PHAkt recruitment (**Supplementary Fig. 9e**) in individual cells by providing the appropriate input to the controller.

Last, we used optogenetic control of PI3K activity to address whether 3′ phosphoinositide lipid amounts can be clamped in cells undergoing the large positive and negative changes in PI3K activity that may result from positive and negative feedback loops acting to shape pathway dynamics. We spiked in LY294002 (PI3K inhibitor) or serum (PI3K-activating input) either in the presence or in the absence of feedback control on PHAkt-Cerulean membrane levels (**Fig. 3b**). As expected, LY294002 addition decreased 3′ phosphoinositide lipid amounts in cells exposed to a constant light input (**Fig. 3c**). However, our controller compensated for pharmacological inhibition of PI3K, maintaining constant 3′ phosphoinositide lipid levels by dramatically increasing the 650-nm light input (**Fig. 3c**) and thus PI3K recruitment. Similarly, after serum-mediated activation of endogenous PI3K, the controller clamped 3′ phosphoinositide lipid amounts by decreasing the light-gated PI3K input (**Fig. 3d** and **Supplementary Fig. 9e–g**).

Here we combined approaches from optogenetics, control theory and cell biology to drive precise patterns of intracellular activity in live cells. Our approach suggests several classes of quantitative live-cell experiments. Time-varying inputs, which have been applied extracellularly to dissect sensory signaling cascades, can now be applied to intracellular signals. Applying control on multiple signaling nodes from a single optogenetic input could be used to 'walk down' a pathway to identify sources of ultrasensitivity or points of feedback connection. Finally, clamping light-gated inputs against cellular changes in activity could be used to disconnect intracellular feedback circuits without genetic or pharmacological perturbation.

METHODS

Methods and any associated references are available in the online version of the paper at http://www.nature.com/naturemethods/.

Note: Supplementary information is available on the Nature Methods website.

ACKNOWLEDGMENTS

We thank all members of the Weiner and Lim laboratories, A. Levskaya, A. Edelstein and N. Stuurman for helpful comments and discussions, and A. Loewer and H. El-Samad for critically reading this manuscript. TagBFP construct was a gift from members of the Vale lab (University of California San Francisco), pHR lentiviral vectors were provided by J.R. James (University of California San Francisco), and the iSH construct was a gift from members of the Meyer lab (Stanford University). This work was supported by a Cancer Research Institute Postdoctoral Fellowship to J.E.T., an American Cancer Society postdoctoral fellowship to D.G., the Howard Hughes Medical Institute and US National Institutes of Health grants GM55040, GM62583, EY016546 and P50GM081879 to W.A.L., and a National Institutes of Health grant GM084040 and a Searle Scholars Fellowship to O.D.W.

AUTHOR CONTRIBUTIONS

J.E.T. conceived and implemented the feedback controller. O.D.W. and W.A.L. supervised the project. All authors designed experiments, which J.E.T. and D.G. performed. J.E.T. analyzed data. J.E.T., W.A.L. and O.D.W. wrote the paper, which all authors edited.

COMPETING FINANCIAL INTERESTS

The authors declare no competing financial interests.

Published online at http://www.nature.com/naturemethods/.
Reprints and permissions information is available online at http://www.nature.com/reprints/index.html.

1. Mettetal, J.T., Muzzey, D., Gomez-Uribe, C. & van Oudenaarden, A. *Science* **319**, 482–484 (2008).
2. Muzzey, D., Gómez-Uribe, C.A., Mettetal, J.T. & van Oudenaarden, A. *Cell* **138**, 160–171 (2009).
3. Shimizu, T.S., Tu, Y. & Berg, H.C. *Mol. Syst. Biol.* **6**, 382 (2010).
4. Hodgkin, A.L., Huxley, A.F. & Katz, B. *J. Physiol. (Lond.)* **116**, 424–448 (1952).
5. Visscher, K., Schnitzer, M.J. & Block, S.M. *Nature* **400**, 184–189 (1999).
6. Rockwell, N.C., Su, Y.S. & Lagarias, J.C. *Annu. Rev. Plant Biol.* **57**, 837–858 (2006).
7. Khanna, R. *et al. Plant Cell* **16**, 3033–3044 (2004).
8. Levskaya, A., Weiner, O.D., Lim, W.A. & Voigt, C.A. *Nature* **461**, 997–1001 (2009).
9. Shimizu-Sato, S., Huq, E., Tepperman, J.M. & Quail, P.H. *Nat. Biotechnol.* **20**, 1041–1044 (2002).
10. Tyszkiewicz, A.B. & Muir, T.W. *Nat. Methods* **5**, 303–305 (2008).
11. Leung, D.W., Otomo, C., Chory, J. & Rosen, M.K. *Proc. Natl. Acad. Sci. USA* **105**, 12797–12802 (2008).
12. Edelstein, A., Amodaj, N., Hoover, K., Vale, R. & Stuurman, N. *Curr. Protoc. Mol. Biol.* **92**, 14.20.01–14.20.17 (2010).
13. Suh, B.C., Inoue, T., Meyer, T. & Hille, B. *Science* **314**, 1454–1457 (2006).
14. Haugh, J.M., Codazzi, F., Teruel, M. & Meyer, T. *J. Cell Biol.* **151**, 1269–1280 (2000).

ONLINE METHODS

Plasmids and constructs. For the PIF-BFP construct, the gene encoding PIF was PCR-amplified from pAL175 (ref. 8) and subcloned with *TagBFP* into the pMSCV-neomycin retroviral vector (Clontech) using custom-designed overhangs using AarI (Fermentas). All other plasmids used the pHR as the lentiviral backbone. For the Phy construct, the mammalian codon–optimized sequences encoding PhyB, mCherry and the CAAX from KRas fusion were subcloned into the pHR lentiviral vector backbone using MluI and XhoI. For the iSH2-YFP-PIF construct, the sequence encoding interSH2 domain from p85 was PCR-amplified from *CF-iSH* and was enzymatically assembled[15] with sequences encodingYFP and PIF into pHR. Similarly, the sequence encoding the PH domain from Akt was enzymatically assembled with *Cerulean* into pHR to make the PHAkt-Cerulean probe.

Retroviral constructs were transfected with TransIT-293 (Mirus Bio) into 293-GPG cells[16] (which stably express the required packaging proteins to produce retrovirus) that had been plated at 70% confluency in 6-cm dishes. After transfection, medium was changed twice; first 16 h after transfection and again 48 h after transfection. Retroviral supernatant was collected 72 h after transfection. All lentiviruses were produced by transfecting pHR-based plasmids along with the vectors encoding packaging proteins (pMD2.G and p8.91) using TransIT-293 into HEK-293 cells at ~70% confluency in six-well plates. Viral supernatants were collected 2 d after transfection. Both retroviruses and lentiviruses were used for transduction immediately or stored at 4 °C for up to 2 weeks.

Retroviral and lentiviral transduction. NIH-3T3 cells (American Type Culture Collection; ATCC) were cultured in 10% bovine calf serum (University of California San Francisco Cell Culture Facility) in DMEM (Invitrogen) supplemented with penicillin, streptomycin and glutamine at 37 °C with 5% CO_2 in a humidified incubator. For viral transduction, NIH-3T3 cells were plated in six-well dishes to achieve ~70% confluency at the time of infection. Viral supernatants were passed through a 0.22-µm filter to exclude dead cells and particulate matter. For lentiviral transduction, 1 ml of viral supernatant was added directly to cells. For retroviral transduction, the viral supernatant was supplemented with 8 µg ml^{-1} of polybrene (Sigma). Viral medium was replaced with normal growth medium 24 h after infection. For cell lines stably expressing multiple signaling components, viral transductions were performed sequentially: first with virus encoding Phy, then with that encoding PIF and then with that encoding PHAkt-Cerulean. Cells were then sorted on a FACsAria2 (Beckton-Dickinson) to enrich for Phy-, PIF- and PHAkt-expressing cells.

Preparing cells for imaging. For imaging experiments, 35-mm glass-bottom Petri dishes (MatTek) were coated for 1 h with 0.08 mg ml^{-1} fibronectin (which we prepared from whole porcine blood) and then washed twice with PBS (pH 7.2). We plated 180,000 cells on each dish in normal growth medium and allowed them to adhere for at least 30 min. For PIF-BFP experiments, we incubated cells for 30 min in a solution of 4 µM phycocyanobilin (PCB, extracted from Spirulina (Spectrum Chemicals)[17]; 4 mM stock was prediluted into conditioned medium and added to dishes in the dark or under a green safelight). PCB-containing medium was then replaced with imaging medium consisting of 2% (v/v) FBS (Invitrogen) in mHBSS (150 mM NaCl, 4 mM KCl, 1 mM $MgCl_2$, 10 mM glucose and 20 mM Hepes; pH 7.2).

For PI3K-recruitment experiments, cells were serum-starved for at least 3 h in 2% w/v fatty acid–free BSA (Sigma) in DMEM. Cells were incubated with PCB for at least 30 min before exchanging into imaging medium (2% (w/v) fatty acid–free BSA in mHBSS).

Microscopy. To tune light inputs for optogenetic control, we used one 650-nm LED and two 750-nm LEDs (Lightspeed Technologies). For these devices, light emission intensity scales linearly with applied voltage (from 0 V to 5 V). To apply light inputs specifically to defined regions of the cell, we used a custom dual-input digital micromirror device (DMD; Andor Technologies). 'On' pixels (regions to be stimulated with activating light) were illuminated with both 650-nm and 750-nm light, whereas 'off' pixels were exposed to the second 750-nm light source at a constant intensity. To implement software-based voltage control of light intensity, we connected both 'on' pixel LEDs to the analog outputs of a DT9812 board (Data Translation) and set their voltages using custom Matlab code (**Supplementary Software**).

Images for light recruitment assays were taken at room temperature on a Nikon Eclipse Ti inverted microscope equipped with a motorized laser total internal reflection fluorescence (TIRF) illumination unit, a 100X PlanApo TIRF 1.49 numerical aperture (NA) objective, and an electron multiplying charge-coupled device (EM-CCD) camera (Evolve, Photometrics). For excitation, 405 nm, 440 nm, 488 nm, 514 nm and 561 nm laser wavelengths (LMM5, Spectral Applied Research) were used.

Our Nikon Eclipse Ti microscope has two stacked dichroic turrets, which we used to achieve independent control of both light stimulation and measurement. The upper turret contained a 620 nm short-pass filter for exposing cells to the DMD light or was left empty (non-DMD imaging). The lower turret contained the TIRF imaging dichroics (Chroma) and was used to deliver the TIRF laser lines. In addition to the shortpass dichroic's rejection of 650-nm and 750-nm light, we used a 625 nm sputtered shortpass emission filter (Chroma) to block DMD light from the camera when acquiring TIRF membrane fluorescence images. Thus, imaging could be performed while cells were simultaneously stimulated with combinations of activating (650 nm) and inactivating (750 nm) light. The microscope, dichroic positions, filters, camera and lasers were all controlled using the open-source Micro-Manager software package (University of California San Francisco) using custom Matlab code (**Supplementary Software**).

Image processing. We removed the short-pass emission filter from the light path to identify the precise location of the 9 µm × 9 µm square 'on' pixel region illuminated by the DMD (**Fig. 1d**). The location of this region was automatically identified using standard image processing tools (Sobel edge detection, image dilation to find horizontal and vertical lines, and hole-filling to identify the closed square region) in the Matlab Image Processing toolbox. Recruitment was quantified as the mean intensity of pixels in the 'on' pixel region.

For some analyses it was useful to consider the normalized recruitment level for an individual cell. In these cases, we used measurements of the mean fluorescence in response to 1-V, 750-nm

doi:10.1038/nmeth.1700

illumination as the minimum fluorescence (F_{min}). Conversely, the mean intensity in the presence of 1 V, pure 650-nm illumination was used as the maximum recruitable fluorescence (F_{max}). Normalized recruitment was computed as

$$F_{norm} = \frac{F - F_{min}}{F_{max} - F_{min}}.$$

For analyses in which background-subtracted fluorescence values were used, we subtracted the minimum fluorescence F_{min} from each fluorescence measurement F using the formula

$$F_{sub} = F - F_{min}.$$

Optimizing imaging conditions for data acquisition and feedback control. Although the peak wavelengths affecting PhyB photoisomerization are in the red to infrared range, both PhyB states are also capable of absorbing light at other frequencies. To ensure that our imaging conditions do not perturb the Phy activity state, we measured the effect on PhyB photoisomerization and PIF recruitment binding in response to various imaging excitation wavelengths. We exposed cells expressing PIF-YFP and Phy-mCherry-CAAX to laser light at five illumination wavelengths and compared to the recruitment elicited by our 650-nm light source. We found that a 30-s exposure to green, yellow and red fluorescent protein imaging wavelengths (488 nm, 514 nm and 561 nm, respectively) led to an increase in PIF-YFP membrane recruitment, where the effect was more pronounced at longer wavelengths (**Supplementary Fig. 1a**). It should be noted that this experiment represents a worst-case scenario, as 30-s exposures are much longer than those delivered during normal imaging (typically 100 ms per acquired image) and no 750-nm light is present to counteract imaging-based activation of PhyB. Although GFP and YFP fluorophores can still be used for quantitative imaging of the Phy-PIF system under conditions of low excitation light levels, the frequent imaging required for feedback control makes these undesirable choices for this work.

In contrast, CFP and BFP imaging wavelengths (440 nm and 405 nm, respectively) had no measurable effect on the Phy-PIF interaction. Thus, for all subsequent experiments involving frequent imaging (such as those implementing feedback control), we imaged CFP- and BFP-based fluorophores. We also verified that frequent BFP imaging does not affect either the steady state or transient response of the Phy-PIF module (**Supplementary Fig. 1b**).

Implementing any feedback-control strategy requires frequent sampling of the system's output to make the appropriate input adjustments. To this end, we sought to identify conditions under which acquiring frequent TIRF images would not lead to fluorophore photobleaching. We could acquire nearly 400 PIF-BFP TIRF images without appreciably affecting the minimal or maximal range of recruitment (**Supplementary Fig. 1c**).

15. Gibson, D.G. *et al. Nat. Methods* **6**, 343–345 (2009).
16. Ory, D.S., Neugeboren, B.A. & Mulligan, R.C. *Proc. Natl. Acad. Sci. USA* **93**, 11400–11406 (1996).
17. Toettcher, J.E., Gong, D., Lim, W.A. & Weiner, O.D. *Methods Enzymol.* **497**, 409–423 (2011).